

A modified Ising model for the thermodynamic properties of local and global protein folding–unfolding observed by circular dichroism and small-angle X-ray scattering

Ying-Jen Shiu,^{a*} U-Ser Jeng,^b Charlene Su,^a Yu-Shan Huang,^b Michitoshi Hayashi,^c Kuo-Kan Liang,^a Yu-Lin Yeh^a and Sheng-Hsien Lin^a

^aInstitute of Atomic and Molecular Sciences, Academia Sinica, Taiwan, ^bNational Synchrotron Radiation Research Center, Taiwan, and ^cCenter for Condensed Matter Sciences, National Taiwan University, Taiwan. Correspondence e-mail: yingjen@gate.sinica.edu.tw

Based on the mean-field approximation, we have applied a modified Ising model to describe general protein unfolding behavior at thermodynamic equilibrium with the free energy contributed by the subgroup units (amino acids or peptide bonds) of the protein. With the thermodynamic properties of the protein, this model can associate the stepwise change of an unfolding fraction ratio profile with the local and global conformation unfolding. Taking cytochrome *c* (cyt *c*) as a model protein, we have observed, using small-angle X-ray scattering and circular dichroism (CD), the global and local structure changes for the protein in three kinds of denaturant environments: acid, urea and guanidine hydrochloride. The small-angle X-ray scattering and CD results are mapped to the unfolding fractions as a function of the pH value or denaturant concentration, from which we have extracted local and global unfolding free energies of cyt *c* in different denaturant environments using a modified Ising model. Based on the characteristics of the thermodynamic properties deduced from the local and global protein folding–unfolding, we discuss the thermodynamic stabilities of the protein in the three denaturant environments, and the possible correlation between the global conformation change of the protein and the local unfolding activities of the S–Fe bond in the Met80-heme and the α -helices.

© 2007 International Union of Crystallography
Printed in Singapore – all rights reserved

1. Introduction

The application of small-angle X-ray scattering (SAXS) is advantageous in the study of the global conformation changes of proteins during folding and unfolding in solution (Durchschlag *et al.*, 1991; Kataoka *et al.*, 1993; Doniach, 2001; Cinelli *et al.*, 2001; Akiyama *et al.*, 2002). The determination of the structural characteristics of proteins is crucial in understanding partially folded or misfolded proteins that are related to many human diseases (Riek *et al.*, 1996; Dobson, 2001; Dill & Chan, 1997). It is generally believed that the three-dimensional structure of a native protein is determined by thermodynamics. In other words, the native state of a protein is a thermal equilibrium state. Many theoretical models have been proposed to describe the three-dimensional structure of a protein folding from the amino-acid sequence under a given thermodynamic environment (Plaxco *et al.*, 1998; Muñoz *et al.*, 1997; Muñoz & Eaton, 1999; Liang *et al.*, 2003*a,b*). To examine the validity of the model proposed, one of the approaches is to change the environment influencing the thermodynamic properties of a protein using denaturant agents, and observe the global and local protein conformation changes by, for instance, SAXS or circular dichroism (CD).

In this work, based on the mean-field approximation (MFA), we have developed a modified Ising model to describe general protein unfolding behavior at thermodynamic equilibrium with the free

energy contributed by the subgroup units (local amino acids or peptide bonds) of a protein. In particular, this model allows us to explain the multiple-stepwise change of the unfolding fraction ratio *via* the individual subgroup unit activities inside a protein. To observe the thermodynamic properties associated with the global and local conformations of a model protein, cytochrome *c* (cyt *c*), we studied the global conformation change of cyt *c* in an unfolding process using SAXS, whereas the α -helix responses recorded in CD spectra revealed information about local structure changes. The stabilities of thermodynamics properties related to the local and global conformations of the protein under three denaturant environments [acid, urea and guanidine hydrochloride (GuHCl)] are discussed in terms of the modified Ising model.

2. Models

2.1. Thermodynamic model – Ising model and MFA

To describe protein folding–unfolding processes, we have developed a modified Ising model from a quantum mechanics point of view (Liang *et al.*, 2003*a,b*). The modified model regards a protein as a collection of subgroup units that can cluster in several groups. More specifically, the groups can be α -helices and/or β -sheets formed by subgroup units such as peptide bonds or amino-acid residues as the

constituent units. Two states, folded and unfolded, are assigned to each unit and noted with a binary variable $\sigma = 1$ or $\sigma = -1$. For M groups in the protein and N_ℓ units in the ℓ th group, a state of the protein can be described by a topological representation of $\{\sigma\} \equiv \{\{\sigma\}_1, \dots, \{\sigma\}_\ell, \dots, \{\sigma\}_M\}$, where $\{\sigma\}_\ell \equiv \{\sigma_1^{(\ell)}, \dots, \sigma_{N_\ell}^{(\ell)}\}$. The fold structure of the protein is regarded as all units being in the folded state $\{\{1, 1, \dots, 1\}_1, \dots, \{1, 1, \dots, 1\}_M\}$, and a fully unfolded structure as all units being in the unfolded state $\{\{-1, -1, \dots, -1\}_1, \dots, \{-1, -1, \dots, -1\}_M\}$. With the unit energy ε_i and the coupling energy $J_{i,j}$ between the units i and j , the total energy of a unit in the system should be $E_i = \varepsilon_i + 2J_{i,j}\sigma_i$. The Hamiltonian can be a summation over the energy of all units in the protein,

$$H(\{\sigma\}) = \sum_{\ell} \sum_{i \in \ell} -\sigma_i^{(\ell)} E_i^{(\ell)}(\{\sigma\}_\ell). \quad (1)$$

In the MFA, the units are presumed identical within the same group, and different groups can have different units. A non-binary value of $\langle \sigma^{(\ell)} \rangle^{\text{eq}}$ in the ℓ th group obtained after taking a thermal average for a canonical ensemble of proteins is given by

$$\langle \sigma^{(\ell)} \rangle^{\text{eq}} = \tanh \left(\frac{\langle E^{(\ell)} \rangle^{\text{eq}}}{k_B T} \right), \quad (2)$$

where k_B is Boltzmann's constant, T is the temperature, and the energy of a unit in the ℓ th group is $\langle E^{(\ell)} \rangle^{\text{eq}} = 2\varepsilon^{(\ell)} + 2J^{(\ell)} \langle \sigma^{(\ell)} \rangle^{\text{eq}}$, and the coupling energy between the nearest neighbor units is $J^{(\ell)} = J_{i,i+1}^{(\ell)} = J_{i,i-1}^{(\ell)}$. The unfolding fraction ratio $f_u^{(\ell)}$ of the unit is given by

$$f_u^{(\ell)} = \frac{1}{1 + \exp \left\{ \left[2\varepsilon^{(\ell)} + 4J^{(\ell)} (1 - 2f_u^{(\ell)}) \right] / k_B T \right\}}, \quad (3)$$

where $\langle \sigma^{(\ell)} \rangle^{\text{eq}} = 1 - 2f_u^{(\ell)}$, and $\Delta G^{(\ell)} = 2\varepsilon^{(\ell)} + 2m\Delta\Delta\varepsilon^{(\ell)}$ is the free energy as a function of the denaturant concentration m . Here, $2\Delta\varepsilon_0^{(\ell)} = \Delta G_0^{(\ell)}$ is the free energy of the protein dissolved in water and $2\Delta\Delta\varepsilon^{(\ell)} = \Delta\Delta G^{(\ell)}$ is the denatured energy per mole for the protein in a denaturant. Therefore, the unfolding fraction ratio $\text{Obs}(m)$ observed in measurements, being a summation over $f_u^{(\ell)}$ of the observed groups with a weighting parameter $\gamma^{(\ell)}$, can be given by

$$\text{Obs}(m) = \sum_{\ell} \gamma^{(\ell)} f_u^{(\ell)}(m), \quad (4)$$

where $\sum_{\ell} \gamma^{(\ell)} = 1$ and $\gamma^{(\ell)} = N_\ell \zeta^{(\ell)} / \sum_{\ell} N_\ell \zeta^{(\ell)}$. Here $\zeta^{(\ell)}$ is the observable, such as the absorption coefficient, M' denotes the number of the groups observed in the measurements, $f_u^{(\ell)}(0) = 0$, and $f_u^{(\ell)}(\infty) = 1$. In this case, the free energy per unit governing the global or local structure changes of a protein can be deduced *via* the observed unfolding fraction ratios in equation (4).

To illustrate the characteristics of equation (4), we performed numerical simulations of the unfolding fraction ratio of a protein consisting of two groups. Fig. 1(a) shows three cases of $\text{Obs}(m)$ with the $\Delta\Delta\varepsilon^{(2)}$ values of (1) $-3.0k_B T$, (2) $-1.5k_B T$, and (3) $-1.2k_B T$, together with the fixed parameters of $\Delta\Delta\varepsilon^{(1)} = -1.0k_B T$, $\gamma^{(1)} = \gamma^{(2)} = 0.5$, $\varepsilon_0^{(1)} = \varepsilon_0^{(2)} = 7.0k_B T$, and $J^{(1)} = J^{(2)} = 0$. In Fig. 1(a), a distinct multiple-stepwise structure is observed for case (1) with the largest difference in $\Delta\Delta\varepsilon^{(1)}$ and $\Delta\Delta\varepsilon^{(2)}$, whereas the multiple-stepwise structure approaches a single-stepwise profile when the difference between the denatured energies of the two groups becomes small, as demonstrated in case (3), and the profile can be well approximated by a single-stepwise profile of one reduced group of $\varepsilon_0 = 5.39k_B T$, $\Delta\Delta\varepsilon = -0.84k_B T$, and $J = 0$ as shown in Fig. 1(b).

In the above demonstrations, we have shown that grouping the folding-unfolding units can generate discontinuous changes in the

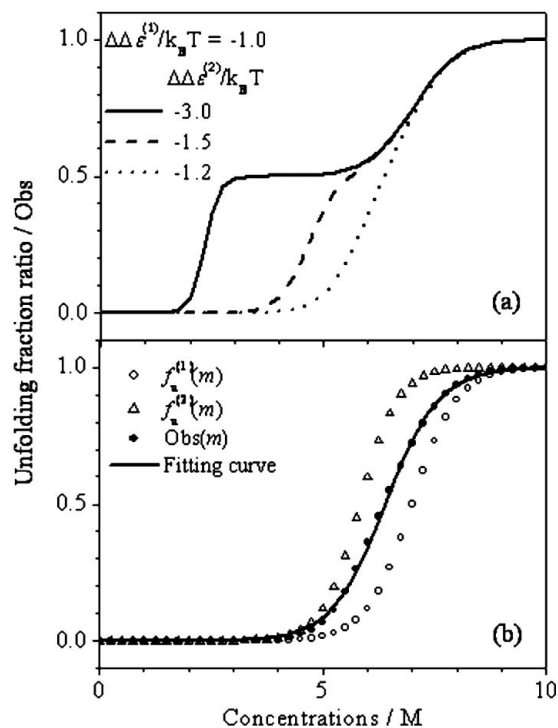


Figure 1 The simulated $\text{Obs}(m)$ for a protein consisting of two groups. Given in (a) are the profiles simulated with three $\Delta\Delta\varepsilon^{(2)}$ values of $-3.0k_B T$ (solid line), $-1.5k_B T$ (dashed line), and $-1.2k_B T$ (dotted line), with fixed $\Delta\Delta\varepsilon^{(1)} = -1.0k_B T$ and equal weighting parameters of $\gamma^{(1)} = \gamma^{(2)} = 0.5$. (b) The last case in (a) (solid circles), contributed from $f_u^{(1)}(m)$ (circles) and $f_u^{(2)}(m)$ (triangles) of the two groups of close free energies, is approximated by the $\text{Obs}(m)$ of one reduced group (solid line).

unfolding fraction ratio, which provides another point of view in interpreting the stepwise structural changes in protein unfolding, which, otherwise, are often explained by an intermediate state in the literature (Doniach, 2001). Moreover, a multiple-stepwise unfolding fraction ratio can be observed if more than two unfolded groups of distinct denatured energies exist in the protein.

Since the structure of an unfolded unit in a protein is associated closely with the denaturant, the unfolded structure of the units, thus, the final unfolded structure of a protein, is not necessary the same in different denaturant environments. Prediction of the exact unfolded protein structure under a specific environment is out of the scope of our present model. However, the unfolding fraction ratio derived from the model can provide the thermodynamic properties of a protein at a given denaturant environment.

2.2. SAXS model

The SAXS profile of a protein dispersed in aqueous solution with no interaction (or interference) can be described by $I(Q) = I_0 \tilde{P}(Q)$, where $\tilde{P}(Q)$ is the normalized form factor, with $\tilde{P}(0) = 1$ (Bendouch *et al.*, 1983; Chen, 1986), and the modulus of scattering vector $Q = (4\pi/\lambda) \sin \theta$, where the scattering angle is 2θ and the wavelength is λ . The zero scattering intensity $I_0 = CN(f - \rho_s V_{\text{dry}})^2$ is determined by the concentration C , aggregation number N (for non-aggregated proteins $N = 1$), dry volume of protein V_{dry} , scattering length f of the protein, and the scattering-length density ρ_s of the solvent (Chen & Lin, 1987; Wu & Chen, 1988; Feigin & Svergun, 1987). For cyt c with 6593 electrons, $f = 0.18592 \text{ \AA}$, whereas $\rho_s = 9.36 \times 10^{-6} \text{ \AA}^{-2}$ for water.

For a homogeneous ellipsoid with semi-major axis c and semi-minor axis a , the form factor averaged for spatial orientation is given by

$$\tilde{P}(Q) = \int_0^1 \left| \frac{3j_1(v)}{v} \right|^2 d\mu, \quad (5)$$

where $v = Q[c^2\mu^2 + a^2(1-\mu^2)]^{1/2}$ and $j_1(v)$ is the spherical Bessel function of the first order. Fitting SAXS data on an absolute intensity scale (of units cm^{-1}) helps to reduce the uncertainties of the fitted a and c values of the ellipsoid model shape used (Lin *et al.*, 2004).

3. Experimental methods and sample preparation

Sample solutions of horse heart cyt *c* in oxidized form were prepared in 7 mM potassium phosphate buffer solution with concentrations of the denaturants in the following ranges: GuHCl, 0.0–5.0 M, pH = 5.4; urea, 0.0–10.0 M, pH = 7.0; and HCl, pH = 2.0–7.0. The protein was received from Sigma Chemical Company and used without further purification. Two sample concentrations, 7 and 21 mg ml⁻¹, were used for SAXS measurements, and the well overlapped SAXS profiles measured after normalization to the sample concentration indicated little or no aggregation or oligomerization in these two sample solutions. Therefore, the higher concentration was used in the series of sample solutions for better scattering intensity. A concentration effect for cyt *c* unfolding has also been reported previously (Segel *et al.*, 1998). For CD measurements (J715, Jasco Co.), a sample concentration of 20 μM was used.

SAXS measurements were conducted on the BL01B beamline at the National Synchrotron Radiation Research Center (NSRRC) (Jeng *et al.*, 2005). With a 1 mm diameter beam (15 keV X-rays) and a sample-to-detector distance of 1.4 m, SAXS data were collected using a 50 mm linear detector. To avoid aggregation due to X-ray irradiation, the samples sealed between 5 mm diameter Kapton windows at 303 K were constantly moved over an area of $2 \times 2 \text{ mm}^2$ during the data collection. The sample thickness was controlled to be within the range 7–3 mm, depending on the denaturant used, for an optimum sample transmission of 0.37.

4. Results and discussion

4.1. Dimensions and envelopes of proteins

Fig. 2 displays the representative SAXS data for the native cyt *c* and the protein denatured by pH = 2 acid, 3.6 M GuHCl, and 10 M urea. The SAXS profiles change drastically at 3.6 M GuHCl and 10 M urea, indicating that in both environments the conformation of the unfolded protein differs significantly from that of the native state. Using the ellipsoid model described previously, we can fit all the SAXS data of cyt *c* in the three denaturants reasonably well. The parameters c and a fitted for the semi-major and semi-minor axes of the ellipsoidal envelope are summarized in Fig. 3. From the fitting results, we find that the semi-major axis c elongates as the denaturant concentration increases, whereas the semi-minor axis a stays roughly the same length. The results suggest that a globular native cyt *c* may be gradually unfolded along a preferred direction as the denaturant concentration increases, starting from a sphere-like shape with an aspect ratio $c/a \approx 1$ for native cyt *c* to an ellipsoid-like shape of $c/a \approx 6.6$ in 3.6 M GuHCl, $c/a \approx 6.0$ in 10 M urea, or $c/a \approx 1.8$ at pH = 2.0 (see Fig. 3). The semi-major axis c of the unfolded cyt *c* in acid at pH = 2.0 is found to be about 1/3 of that in 3.6 M GuHCl and 10 M urea.

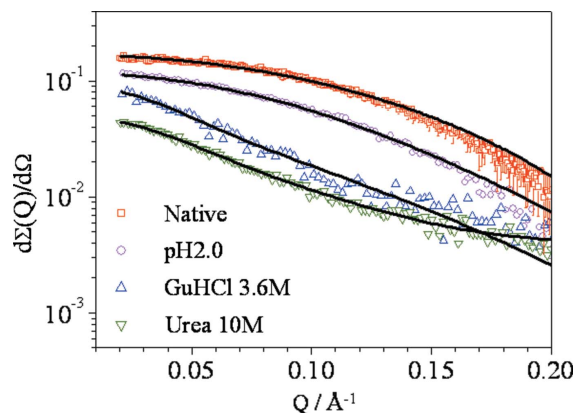


Figure 2
SAXS data for the native cyt *c* at pH = 7.0, and the protein unfolded in the three denaturant environments of acid at pH = 2.0, 3.6 M GuHCl at pH = 5.4, and 10 M urea at pH = 7.

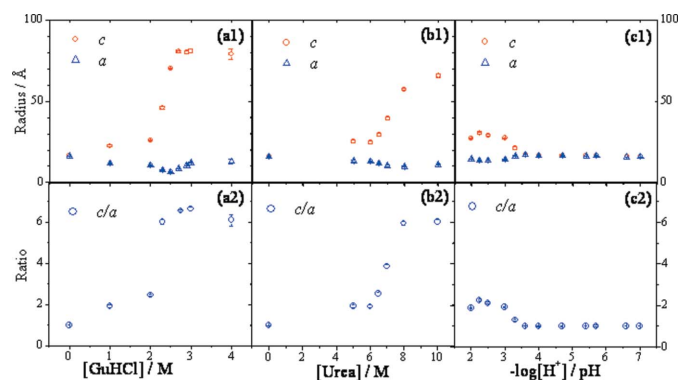


Figure 3
The fitted c and a values of the ellipsoid model and the deduced aspect ratio c/a of cyt *c* as a function of the concentration of the three denaturants: (a) GuHCl, (b) urea, and (c) acid.

For a consistency check on the ellipsoid model shape used in the SAXS data fitting, we have also performed a dummy residue simulation for the SAXS data measured (Svergun *et al.*, 2001; Koch *et al.*, 2003). As shown in Fig. 4, the elongated envelopes obtained for the unfolded cyt *c* in 2.75 M GuHCl from the simulation are essentially consistent with the ellipsoidal shape fitted previously. Particularly, both methods indicate that the aspect ratio of the protein changes from ~ 1 for the native structure to ~ 6.6 for the unfolded conformation.

4.2. Local and global unfolding of the protein

In this section, global unfolding information for the protein observed previously by SAXS is associated with the local group unfolding of α -helices obtained from the CD spectra. Regarding α -helices as a single group in cyt *c*, the observed CD data are fitted to equation (4) to extract the values of ΔG_0 , $\Delta\Delta G$, and J with $\gamma = 1$. The thermodynamic properties thus deduced are listed in Table 1, together with the concentration C_m deduced at an equilibrium rate constant $K_{\text{eq}} = 1$ where $f_u = 0.5$. As shown in the table, ΔG_0 is about 6.9 kcal mol⁻¹ in GuHCl, 10.2 kcal mol⁻¹ in urea, and 11.4 kcal mol⁻¹ in acid (where 1 kcal mol⁻¹ = 4.184 kJ mol⁻¹). Furthermore, the corresponding values for $\Delta\Delta G$ are -2.9, -1.4, and -3180 kcal mol⁻¹ M⁻¹, respectively. The averaged coupling energy J is -1.35 kcal mol⁻¹ in acid, and is almost negligible in the other two

Table 1

The deduced values of C_m , free energy ΔG_0 , denatured energy per mole $\Delta\Delta G$, and the coupling J of the local sites α -helices and the global envelope of cyt c.

Group	Agent	C_m (M)	ΔG_0 (kcal mol ⁻¹)	$\Delta\Delta G$ (kcal mol ⁻¹ M ⁻¹)	J (kcal mol ⁻¹)
α -helices	GuHCl	2.4	6.90 ± 0.05	-2.90 ± 0.05	0.00 ± 0.05
	Urea	7.3	10.20 ± 0.05	-1.40 ± 0.05	0.00 ± 0.05
	[H ⁺] [†]	10 ^{-2.4}	11.40 ± 0.05	-3180 ± 5	-1.35 ± 0.05
Volume	GuHCl	3.0	17.1 ± 0.1	-6.2 ± 0.1	-0.00 ± 0.05
	Urea	7.8	7.8 ± 0.1	-1.00 ± 0.1	-0.00 ± 0.05
	[H ⁺]	10 ^{-6.0} ‡	3.9 ± 0.1‡	-3992720 ± 50‡	-0.00 ± 0.05‡
	[H ⁺]	10 ^{-3.7} §	3.4 ± 0.1§	-14480 ± 50§	-0.00 ± 0.05§

† Shiu *et al.*, 2004. ‡ First group. § Second group

denaturants. A detailed discussion of the acid effect in protein unfolding has been reported previously (Shiu *et al.*, 2004). Since the stability of the protein against a denaturant can be approximately estimated by the value of $|\Delta G_0/\Delta\Delta G|$, which is directly associated with C_m (a smaller value of $|\Delta G_0/\Delta\Delta G|$ corresponds to a lower thermodynamic stability of the protein), the much smaller value of C_m (10^{-2.8}–10^{-2.4} M) of cyt c in the acid environment (see Table 1) indicates a lower thermodynamic stability of the α -helices of cyt c compared to that in the other denaturant environments.

On the other hand, the unfolding fraction ratio from the global conformation of cyt c may be presented by the volume change of the protein envelope, based on the ellipsoidal shape model of a volume $V = 4\pi ca^2/3$. Fig. 5 presents the unfolding fraction ratio profiles deduced from the volume of the protein envelope and the α -helix response in the CD spectra, denoted by the closed and open circles, respectively. The unfolded secondary structure (the α -helices) is

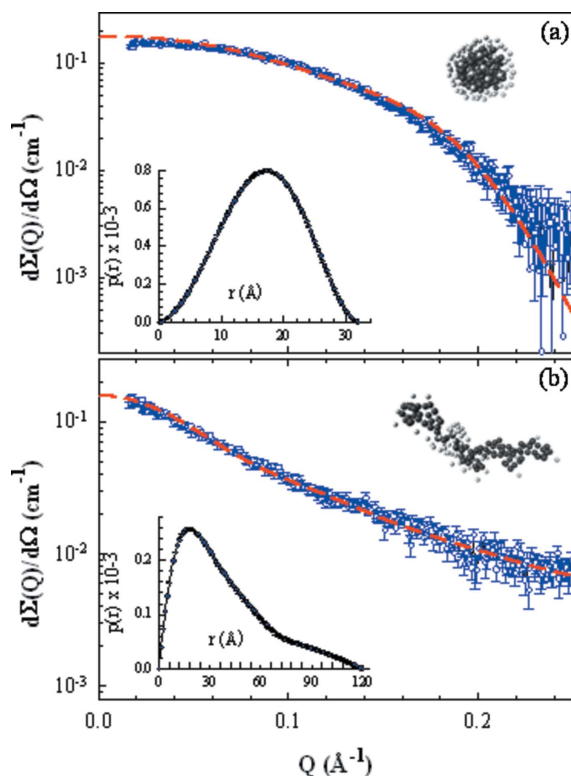


Figure 4 Dummy residue simulations (dashed curves) for the SAXS data of the folded (a) and the unfolded (b) cyt c in 2.75 M GuHCl. Also shown are the corresponding protein envelopes (dark beads) surrounded by a water layer (light beads). The inserts show the $p(r)$ functions Fourier transformed from the respective SAXS data.

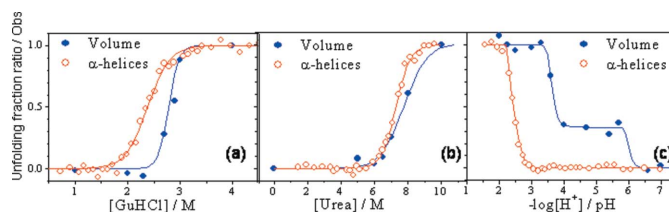


Figure 5 A comparison between unfolding fraction ratios obtained from the local sites responses of α -helices and the global volume response of cyt c in (a) GuHCl, (b) urea, and (c) acid.

commonly considered to be the major contribution to the dimension change in protein unfolding. However, our result shown in Fig. 5 reveals the existence of lags between the α -helix response and the volume response of cyt c to the denaturant concentrations or pH values.

With the modified Ising model, we fitted (solid curves) the profiles of the unfolding fraction ratio in Fig. 5, to get the free energies discussed previously. As a consequence, the unfolding fraction ratio profiles obtained from the global conformation changes of cyt c denatured by urea and GuHCl can be approximated by the unfolding behavior of a reduced single group in the model. The fitted ΔG_0 is 17.7 kcal mol⁻¹ in GuHCl and 7.8 kcal mol⁻¹ in urea, and their corresponding $\Delta\Delta G$ values are -6.2 and -1.0 kcal mol⁻¹ M⁻¹, whereas J is almost negligible. In contrast, cyt c in acid shows a double-stepwise profile of the global unfolding fraction ratio, suggesting that at least two reduced groups with distinguishable free energies are necessary to interpret the global conformation changes of cyt c in acid. From the profile, the first reduced group is unfolded within pH = 3.7–6.0 with $C_m = 10^{-6.0}$, and the second one is unfolded within pH = 2.0–3.7 with $C_m = 10^{-3.7}$. With $\gamma^{(1)} = 0.33$, $\gamma^{(2)} = 0.67$ and $J = 0$, the best-fit values of $\Delta G_0^{(1)}$ and $\Delta G_0^{(2)}$ are 3.9 and 3.4 kcal mol⁻¹, respectively, and $\Delta\Delta G^{(1)}$ is about two orders larger than $\Delta\Delta G^{(2)}$, as listed in Table 1. The smaller C_m value for the second reduced group compared to the C_m value extracted from the CD results suggests a lower thermodynamic stability of the group than the local α -helices when cyt c is denatured by acid. On the other hand, the slightly larger C_m value extracted from the global conformation compared to that from the local α -helices indicates that the global conformation of cyt c can be more thermodynamically stable than the local α -helices in urea and GuHCl environments.

It is reported that the bond strength of the Met80-heme of cyt c becomes weaker at pH < 5.0 because the absorption peak at 695 nm starts to decay at pH = 5.0 (Greenwood, 1976). Based on this result, we associate the Met80-heme with the first reduced group unfolding of cyt c that occurs in acid in the pH range 4.0 < pH < 6.0. From our SAXS and CD results (Fig. 5c), the expanded envelope volume of cyt c resulting from the first reduced group unfolding is ~1.13 times that of the native one, possibly implying the breaking of the Met80-heme, since there are virtually no α -helix unfolding activities observed. Furthermore, when the pH is < 4.0, the local unfolding of α -helices correlates with the stepwise global unfolding, indicating that the α -helices of cyt c in acid may be responsible the second reduced group, and their local unfolding activities result in the further increase of the global aspect ratio of cyt c to ~2.

5. Summary and conclusions

A modified Ising model allowed us to extract the local and global free energies associated with the local and global structure unfolding of cyt c in the three denaturant environments of acid, GuHCl, and urea.

Using an ellipsoid model in the SAXS data analysis, we have extracted global structure information about the protein in the three denaturant environments. The local structural characteristics of the protein, mainly represented by α -helices, have also been revealed by CD spectra. The unfolding fraction ratio of cyt c deduced from SAXS results shows a double-stepwise profile in the acid denaturant environments and single-stepwise profiles in the denaturant environments of GuHCl and urea. The observed double-stepwise profile implies that there are at least two reduced groups in cyt c that can respond individually in the acid environments. We correlate the two groups to the α -helices and the Met80-heme of cyt c. The thermodynamic stability of the Met80-heme is less than that of the α -helix structure in the acid environment; and the α -helix structure in acid is less stable than in the urea and GuHCl environments. The breaking of the Met80-heme may result in an expansion of the volume of cyt c by ~ 1.13 times as compared to that of the native structure. In contrast to the use of an intermediate state to describe the multiple-stepwise conformation changes in protein unfolding, our modified Ising model can describe the same behavior using the concept of folding–unfolding units that form group activities in a protein.

We would like to thank Professor S. H. Chen, Professor S. Takahashi and Dr S. Akiyama for kind discussions and suggestions, and Drs Y. H. Lai and Y. S. Sun for assistance with the SAXS data collection. This work is supported by the NSC of ROC and Academia Sinica.

References

- Akiyama, S., Takahashi, S., Kimura, T., Ishimori, K., Morishima, I., Nishikawa, Y. & Fujisawa, T. (2002). *Proc. Natl Acad. Sci. USA*, **99**, 1329–1334.
- Benedouch, D., Chen, S.-H. & Koehler, W. C. (1983). *J. Phys. Chem.* **87**, 153–159.
- Chen, S. H. (1986). *Ann. Rev. Phys. Chem.* **37**, 351–399.
- Chen, S. H. & Lin, T. L. (1987). *Methods Exp. Phys.* **23**, 489–543.
- Cinelli, S., Spinozzi, F., Itri, R., Finet, S., Garsugli, F., Onori, G. & Mariani, P. (2001). *Biophys. J.* **81**, 3522–3533.
- Dill, K. A. & Chan, H. S. (1997). *Nature Struct. Biol.* **4**, 10–19.
- Dobson, C. M. (2001). *Philos. Trans R. Soc. London Ser. B*, **356**, 133–145.
- Doniach, S. (2001). *Chem. Rev.* **101**, 1763–1778.
- Durchschlag, H., Zipper, P., Wilfling, R. & Purr, G. (1991). *J. Appl. Cryst.* **24**, 811–831.
- Feigin, L. A. & Svergun, D. I. (1987). *Structure Analysis by Small-Angle X-ray and Neutron Scattering*, p. 69. New York: Plenum.
- Greenwood, C. (1976). *Biochem. J.* **153**, 159–163.
- Jeng, U., Hsu, C. H., Sun, Y. S., Lai, Y. H., Chung, W. T., Sheu, H. S., Lee, H. Y., Song, Y. F., Liang, K. S. & Lin, T. L. (2005). *Macromol. Res.* **13**, 506–513.
- Kataoka, M., Hagihara, Y., Mihara, K. & Goto, Y. (1993). *J. Mol. Biol.* **229**, 591–596.
- Koch, M. H. J., Vachette, P. & Svergun, D. I. (2003). *Q. Rev. Biophys.* **36**, 147–227.
- Lin, T.-L., Jeng, U., Tsao, C.-S., Liu, W.-J., Canteenwala, T. & Chiang, L. Y. (2004). *J. Phys. Chem. B*, **108**, 14884–14889.
- Liang, K. K., Hayashi, M., Shiu, Y. J., Mo, Y., Shao, J., Yan, J. & Lin, S. H. (2003a). *J. Chin. Chem. Soc.* **50**, 335–338.
- Liang, K. K., Hayashi, M., Shiu, Y. J., Mo, Y., Shao, J., Yan, J. & Lin, S. H. (2003b). *Phys. Chem. Chem. Phys.* **5**, 5300–5308.
- Muñoz, V., Thompson, P. A., Hofrichter, J. & Eaton, W. A. (1997). *Nature (London)*, **390**, 196–199.
- Muñoz, V. & Eaton, W. A. (1999). *Proc. Natl Acad. Sci. USA*, **96**, 11311–11316.
- Plaxco, K. W., Simons, K. T. & Baker, D. (1998). *J. Mol. Biol.* **277**, 985–994.
- Riek, R., Hornemann, S., Wider, G., Billeter, M., Glockshuber, R. & Wuthrich, K. (1996). *Nature (London)*, **382**, 180–182.
- Shiu, Y. J., Su, C., Liang, K. K., Yeh, Y. L., Hayashi, M. & Lin, S. H. (2004). *J. Chin. Chem. Soc.* **51**, 1161–1173.
- Segel, D. J., Fink, A. L., Hodgson, K. O. & Doniach, S. (1998). *Biochemistry*, **37**, 12443–12451.
- Svergun, D. I., Petoukhov, M. V. & Koch, M. H. J. (2001). *Biophys. J.* **80**, 2946–2953.
- Wu, C. F. & Chen, S. H. (1988). *Biopolymers*, **27**, 1065–1088.